Science of the Total Environment 407 (2009) 3518–3529

Contents lists available at ScienceDirect

Science of the Total Environment

journal homepage: www.elsevier.com/locate/scitotenv

# Aerosol background at two remote CAWNET sites in western China

Wen-Jun Qu [a,b,*], Xiao-Ye Zhang [b], Richard Arimoto [c], Ya-Qiang Wang [b], Dan Wang [d], Li-Fang Sheng [a], Gang Fu [a]

[a] Key Laboratory of Physical Oceanography, Ocean-Atmosphere Interaction and Climate Laboratory, Department of Marine Meteorology, College of Physical and Environmental Oceanography, Ocean University of China, 238 Songling Rd., Laoshan District, Qingdao 266100, China
[b] Key Laboratory of Atmospheric Chemistry, Centre for Atmosphere Watch and Services (CAWAS), Chinese Academy of Metrological Sciences, China Meteorological Administration, 46 Zhong-Guan-Cun S. Ave., Beijing 100081, China
[c] Carlsbad Environmental Monitoring and Research Center, New Mexico State University, Carlsbad, New Mexico, USA
[d] State Key Laboratory of Loess and Quaternary Geology, Institute of Earth Environment, Chinese Academy of Sciences, 10 Fenghui S. Rd., PO Box 17, XiAn 710075, China

ARTICLE INFO

*Article history:*
Received 8 August 2008
Received in revised form 12 December 2008
Accepted 9 February 2009
Available online 9 March 2009

*Keywords:*
Aerosol variation
Regional aerosol background
Baseline
SOC estimation
Remote western China

ABSTRACT

The frequency distributions and some statistical features of background aerosol concentrations were investigated at two remote China Atmosphere Watch Network (CAWNET) stations. The estimated elemental carbon (EC) background at Akdala (AKD) in the mid-latitudes of northwestern China (~0.15 μg $m^{-3}$) was only half of that at Zhuzhang (ZUZ) in low-latitude southwestern China (~0.30 μg $m^{-3}$). The contributions of EC to the aerosol mass also differed between sites: EC contributed 3.5% of the $PM_{10}$ mass at AKD versus 5.1% at ZUZ. Large percentages of the total organic carbon (OC) apparently were secondary organic carbon (SOC); SOC/OC averaged 81% at ZUZ and 68% at AKD. The OC/EC ratios in $PM_{10}$ (ZUZ: 11.9, AKD: 12.2) were comparable with other global background sites, and the OC/EC ratios were used to distinguish polluted periods from background conditions. The $SO_4^{2-}$, $NH_4^+$ and soil dust loadings at AKD were higher and more variable than at ZUZ, probably due to impacts of pollution from Russia and soil dust from the Gobi and adjacent deserts. In contrast to ZUZ, where the influences from pollution were weaker, the real-time $PM_{10}$ mass concentrations at AKD were strongly skew right and the arithmetic mean concentrations of the aerosol populations were higher than their medians. Differences in the aerosol backgrounds between the sites need to be considered when evaluating the aerosol's regional climate effects.



## 1. Introduction

Concerns over climate alteration, visibility impairment, and human health have stimulated interest in understanding how humans have affected the atmospheric aerosol. Knowledge of the aerosol background is not only important for studying the changes in aerosol populations caused by humans but also for assessing the transboundary transport of pollution and for investigating large-scale aerosol effects on climate and biogeochemical cycles. The *aerosol background* is difficult to define rigorously, but it may be thought of as a reasonably stable aerosol population that is representative of a large area and upon which pulses from both natural and pollution sources are occasionally superimposed. A better understanding of the aerosol background also will be helpful in developing effective plans to control pollution emissions, especially $PM_{10}$ (particles ≤10 μm in diameter), a pollutant of primary concern for many Chinese cities.

Observations have been made at atmospheric background sites in China for several decades; most notably at Mt. Waliguan, the global background station in Qinghai Province (Wang et al., 2002; Zhou et al., 2004), and at Mt. Longfengshan, Shangdianzi, and Lin'an, which are located in Heilongjiang, Beijing and Zhejiang, respectively. To the authors' knowledge, however, atmospheric background observations were not made in remote southwestern and northwestern China until 2004 (Qu et al., 2008). The observations to date have mainly targeted gaseous species, and observations of atmospheric aerosols at these background sites have been mostly short-term and mainly involved trace elements and water-soluble (WS) ions (Ma et al., 2003; Wang et al., 2004).

There remains considerable arbitrariness and uncertainty with respect to what constitutes atmospheric background or baseline conditions. Measurements made at sites where the influences of local pollutants are minimal and conditions are reasonably representative of a large area can provide information on this background. However, at the same time large, often episodic, natural emissions coupled with increasing anthropogenic emissions can cause variability in the aerosol even in remote areas of the world. Indeed, a survey of global data has shown that the concentrations and compositions of fine

* Corresponding author. College of Physical and Environmental Oceanography, Ocean University of China, 238 Songling Rd., Laoshan District, Qingdao 266100, China. Tel.: +86 532 66781309; fax: +86 532 66782790.
*E-mail addresses:* quwj@ouc.edu.cn, quwj@163.com (W.-J. Qu).

0048-9697/$ – see front matter. 
doi:10.1016/j.scitotenv.2009.02.012

particles can be highly variable even in areas presumed to be dominated by natural sources (Hidy and Blanchard, 2005).

To assess regional aerosol backgrounds in China, we have conducted studies at two China Atmosphere Watch Network (CAWNET) stations: (1) Zhuzhang (ZUZ) which is located in a mountainous rural area of southwestern China and (2) Akdala (AKD) which is in a hilly area in the northwestern part of the country (Fig. 1). The aerosol composition and influences from regional transport have been described previously (Qu et al., 2008). Here we examine the frequency distributions and variations of the aerosol chemical data and combine that information with estimates of the pollutants' levels for the transport pathways to assess the regional aerosol backgrounds. The objectives of this paper are to (1) evaluate and compare the statistical distribution and variations of the aerosol populations at ZUZ and AKD; (2) estimate the contribution of secondary organic carbon (SOC) to aerosol mass; and (3) estimate the background levels of the aerosol populations at these two sites.

## 2. Methods

The sampling and analytical techniques used for this work have been previously described (Qu et al., 2008), and therefore only a brief description is given below. Measurements of aerosol composition were made at two remote sites, (1) Zhuzhang (ZUZ, 28° 00′ N, 99° 43′ E, 3583 m above sea level, on the southeast margin of the Tibetan Plateau in southwestern China) and (2) Akdala (AKD, 47° 06′ N, 87° 58′ E, 562 m asl, on the north margin of the Zhungaer Basin in northwestern China) (Fig. 1).

Samples included 72-hour (normally from 8:00 to 8:00, local time) bulk $PM_{10}$ samples; these were collected from July 2004 to March 2005 at both sites. Daytime (normally from 8:00 to 20:00, local time) bulk TSP (total suspended particle) aerosol samples also were collected but only at AKD. For the first week of the study at ZUZ and for the first 2 weeks at AKD, 47 mm diameter Teflon® (PTFE) filters (WTP, Whatman Ltd, Maidstone UK) were used for sampling, but 47 mm diameter Whatman quartz microfibre filters (QM/A, Whatman Ltd, Maidstone UK) (preheated at 800 °C for 4 h to remove contaminants) were subsequently used for the measurements. Aerosol mass was determined gravimetrically with the use of an electronic microbalance with 1 μg sensitivity (ME 5-F, Sartorius AG, Goettingen Germany).

Real-time $PM_{10}$ mass concentrations, averaged over 30 min, were determined during the sampling campaign by using a tapered element oscillating microbalance ambient particulate monitor (TEOM® series 1400a, Rupprecht & Patashnick, Albany, NY, US). For these measurements, a 16.7 l/min (lpm) airstream was drawn through a $PM_{10}$ inlet into the instrument, then isokinetically split into 1 lpm and 15.7 lpm airstreams. The 1 lpm airstream was sent to the instrument's mass transducer while the 15.7 lpm airstream led to the sampling unit. Inside the mass transducer, the air stream was filtered by a Teflon®-coated borosilicate glass filter located at the end of an oscillating tapered element. The filter unit was held at 50 °C to prevent condensation. As mass collected on the filter, changes in the oscillations were measured and converted to mass. Measurements were made every 2 s, and those data were integrated to calculate 30-min averages for particulate mass.

The bulk samples were analyzed for organic carbon and elemental carbon (OC and EC) using a DRI Model 2001 Thermal/Optical Carbon Analyzer following the IMPROVE thermal/optical reflectance (TOR) procedure (Chow et al., 1993). Chemical analyses of the water-soluble (WS) ions, including $SO_4^{2-}$, $NO_3^-$, $NH_4^+$, $Ca^{2+}$, $Mg^{2+}$, $K^+$, $Na^+$, $NO_2^-$, $Cl^-$ and $F^-$, were conducted with the use of a Dionex® 600 ion chromatograph (IC) equipped with an ED50A electrochemical detector

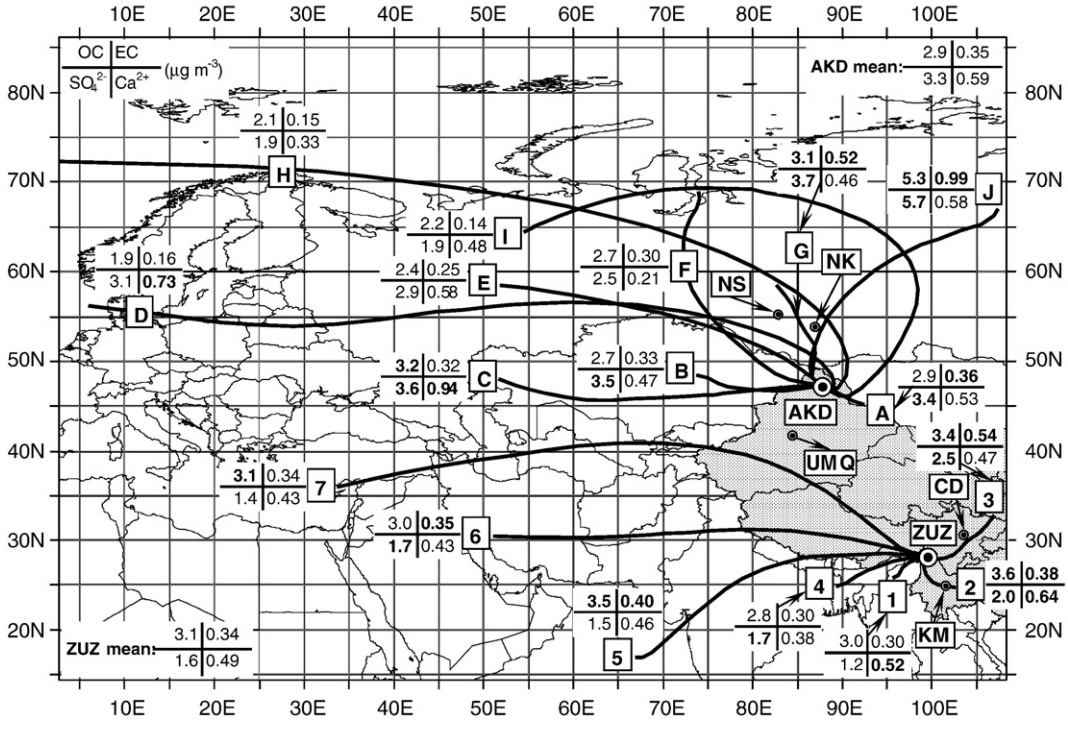


**Fig. 1.** Sampling sites and 5-days backward trajectory clusters for Zhuzhang (ZUZ) (Clusters 1–7) and Akdala (AKD) (Clusters A–J). The shadowed area represents continental China. NK, NS, UMQ, CD and KM denote Novokuznetsk, Novosibirsk, Urumqi, Chengdu and Kunming, respectively. The mean concentrations of organic carbon (OC), elemental carbon (EC), $SO_4^{2-}$ (sulfate) and $Ca^{2+}$ (indicator of soil dust) for the trajectory clusters are also presented; boldface indicated the values higher than the mean of total samples (adapted after Qu et al., 2008). Transport pathways to ZUZ: (1) the polluted, northeasterly Cluster 3 (C-3, from the Sichuan Basin influenced by coal-combustion and mining), and southeasterly C-2 (over southeastern Yunnan Province), (2) the clean, southwesterly C-1 and C-4 (from coasts around Bay of Bengal), (3) the remote clean, southwesterly C-5 (from the Arabian Sea), westerly C-6 (from West Asia), and northwesterly C-7 (from East Europe). Transport pathways to AKD: (1) the major polluted, northeasterly C-J and northwesterly C-G (passing near major Russian industrial cities, NK and NS), and southeasterly C-A (over northwestern Chinese boundary with Mongolia with coal and metal mining), (2) the clean northwesterly C-H, C-I and C-F (from eastern European and Russian high latitudes), (3) the westerly C-B, C-C, C-D and C-E (accounted for 70% the total trajectories and delivered dust).

(Dionex Corp, Sunnyvale, CA, US). The concentrations of trace elements were determined by a proton-induced x-ray emission (PIXE) method; eighteen elements analyzed were As, Br, Ca, Cl, Cr, Cu, Fe, K, Mn, Ni, Pb, S, Se, Sr, Ti, V, Zn, Zr for quartz filters and an additional four elements (Al, Mg, P, Si) for the Teflon® filters. All data were corrected for backgrounds from the average of blank filters (Qu et al., 2008).

To evaluate the aerosol background, we stratified the aerosol data based on trajectory clusters following the methods of Qu et al. (2008). Five-day air-mass backward in time trajectories were calculated with the NOAA HYSPLIT4 trajectory model (Draxler and Hess, 1998) using the NCEP (National Center for Environmental Prediction) FNL (final analysis) meteorological data fields. These trajectories were generated four times each day (00:00, 06:00, 12:00 and 18:00 UTC) and were divided into distinct transport clusters by using trajectory clustering, a multivariate statistical analysis method (Moody and Galloway, 1988; Arimoto et al., 1999). In this method, squared Euclidean distances were used to determine the similarities between the trajectories, and Ward's method was used to make hierarchical clusters of the trajectories. The clustering results are used to evaluate transport to the sampling sites, which are illustrated in Fig. 1.

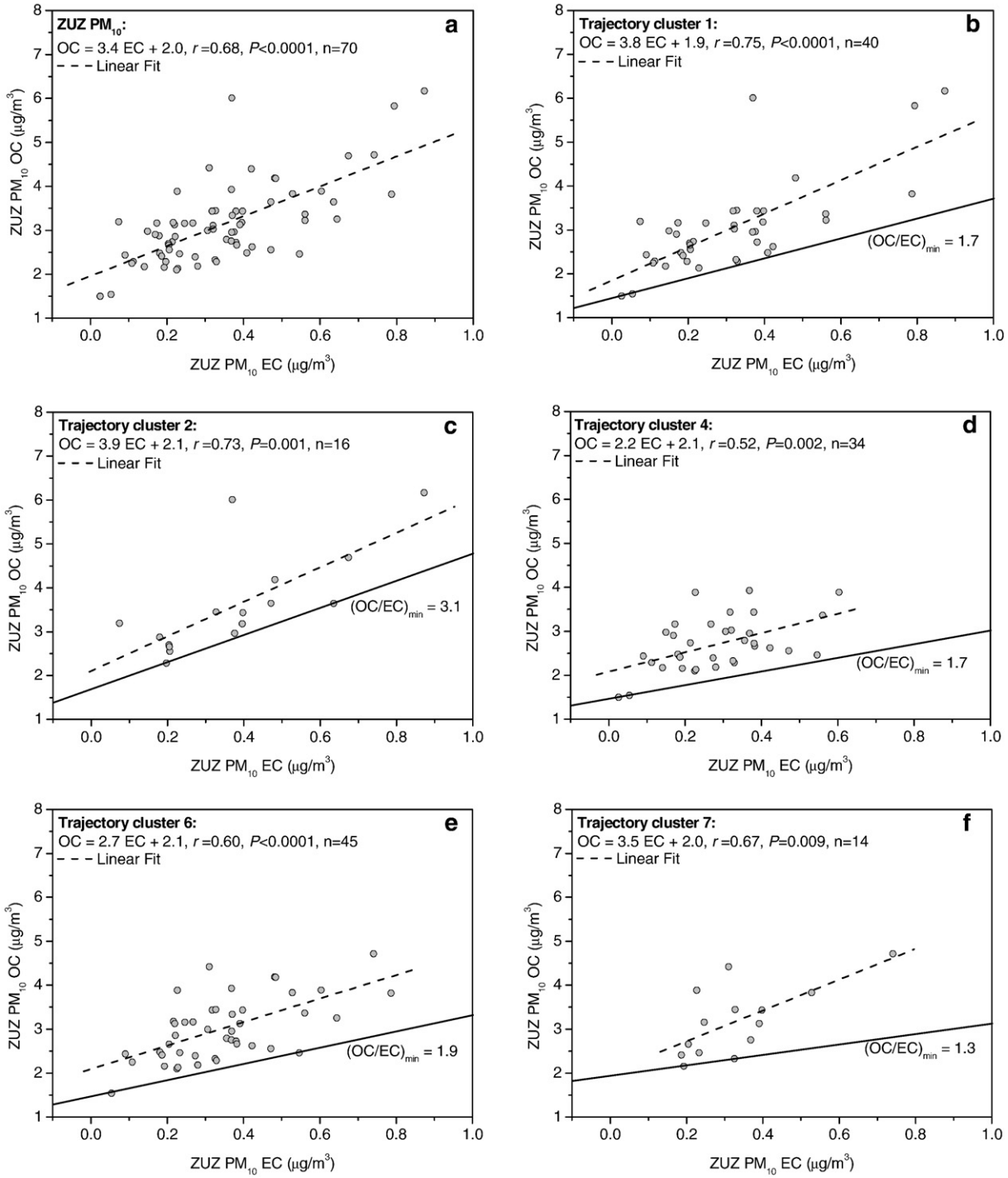


**Fig. 2.** The relationship between $PM_{10}$ organic carbon (OC) and elemental carbon (EC) at Zhuzhang (ZUZ) for (a) all samples; and for the major trajectory clusters: (b) cluster 1, (d) cluster 4, relative clean trajectories from coastal regions near the Bay of Bengal; (c) cluster 2, polluted trajectories from southeastern Yunnan Province; (e) cluster 6, (f) cluster 7, relative clean trajectories from East Europe and West Asia.

## 3. Results and discussion

### 3.1. Similarities in the aerosol populations at Zhuzhang and Akdala

#### 3.1.1. High organic carbon/elemental carbon (OC/EC) ratios

Consistent with is generally seen at remote sites, the OC/EC ratios in $PM_{10}$ were relatively high at both ZUZ and AKD, averaging 11.9 and 12.2, respectively. For comparison, the OC/EC ratio for $PM_{2.5}$ from an agricultural and pasturing area in California averaged $8.1 \pm 2.9$ (Kwangsam et al., 2004), and a ratio of 7.8 for $PM_{2.5}$ was reported for San Nicolas Island during 1995–1996 (Kim et al., 2000). The OC/EC ratios over the Chinese mainland are typically 3 or slightly above (Xu et al., 2002; Cao et al., 2003; Ye et al., 2003; He et al., 2004; Li, 2004; Zhang et al., 2005, 2008; Duan et al., 2005). An OC/EC ratio of 9.0 has been reported by Cachier et al. (1989) for biomass burning aerosols during the dry season at Lamto in the savannah of the Ivory Coast.

OC includes both a primary fraction ($OC_{pri}$) and a secondary fraction (SOC) that forms from precursor gases. On the other hand, EC is assumed to be a primary pollutant and does not form during transport. Therefore high OC/EC ratios can be explained by the formation of SOC or the removal of EC during transport. Consequently, one would expect that in regions lacking strong anthropogenic emissions, OC would be the more abundant form of the carbonaceous aerosol.

Indeed, the OC/EC ratios in the $PM_{10}$ samples from ZUZ and AKD tended to vary inversely with total carbon (TC = OC + EC) concentrations, indicating that the proportions of EC were relatively higher in the more heavily polluted air. At ZUZ, a moderate correlation ($r = 0.68$, $n = 70$) between OC and EC in $PM_{10}$ (Fig. 2a) implies that the two types of carbon compounds were not controlled by the same sources and sinks because the relationship between OC and EC explains less than half of the observed variance.

The formation of SOC combined with OC from biogenic volatile organic compounds (VOCs) evidently contributes to the OC pool in summer and autumn at ZUZ (Qu et al., 2008), and sources such as this would lead to high OC/EC ratios. While the high ratio at AKD may be largely explained by the formation of SOC and removal of EC during transport, there also have been reports of high proportions of OC in the emissions from coal combustion and biomass burning which are major sources for the carbonaceous aerosol in Xinjiang Province (Cao et al., 2006). In related studies, OC has been found to account for 70–80% mass of biomass burning aerosol (Ferek et al., 1998).

In comparison, except for aircraft emissions in the upper troposphere, EC sources are mostly restricted to the earth's surface in populous regions (Highwood and Kinnersley, 2006). The high OC/EC ratio at ZUZ (3583 m asl) suggests that OC may be generally more abundant than EC above the boundary layer in the northern hemisphere. Along these same lines, Hidy and Blanchard (2005) suggested that in many remote areas EC exhibits relatively constant concentrations that are much lower than those of organic matter.

#### 3.1.2. Large secondary organic carbon (SOC) proportions in total OC

As SOC forms during transport but EC does not, OC/EC ratios tend to increase commensurately. However, SOC formation can be slow under certain conditions, such as when solar radiation and ozone are low, there is intermittent or intensive drizzling, the air is unstable, etc. (Turpin and Huntzicker, 1991; Lim, 2001). Under those conditions, the OC/EC ratios can approach those of primary emissions. Based on this notion, the observed minimum OC/EC ratio [$(OC/EC)_{min}$] can be substituted for the characteristic primary emission ratio $(OC/EC)_{pri}$ as a way of estimating the $OC_{pri}$ and SOC as follows:

$$\begin{aligned} SOC &= OC_{total} - OC_{pri} \\ &= OC_{total} - (OC/EC)_{pri} * EC \\ &\approx OC_{total} - (OC/EC)_{min} * EC \end{aligned} \quad (1)$$

where $OC_{total}$ denotes the total OC (Turpin and Huntzicker, 1995; Castro et al., 1999). We use this relationship to estimate SOC concentrations at the two sites below.

*3.1.2.1. Secondary organic carbon at Zhuzhang.* Clear seasonal variations in transport to ZUZ (Qu et al., 2008) along with variations in aerosol sources make it necessary to evaluate SOC concentrations for a variety of transport conditions, which are represented here by the air mass trajectory clusters. Significant correlations ($p < 0.01$ significance) were observed between EC and OC for all samples from ZUZ and for the major trajectory clusters as shown in Fig. 2. Trajectories clusters C-3 and C-5 are not discussed here because the numbers of samples in those groups were small. Variations in $(OC/EC)_{min}$ values can be seen when the data are binned by transport pathways, and we attribute these variations to differences in the emission sources.

For example, the $(OC/EC)_{min}$ for the C-2 trajectories from southeastern Yunnan province was 3.1, the highest of all clusters, and this may be explained by strong VOC emissions and SOC formation in summer and autumn coupled with some impacts from regional biomass burning. The southwesterly C-1 and C-4 trajectories, which also are most common in summer and autumn, pass over areas around the Bay of Bengal, and both had an $(OC/EC)_{min}$ of 1.7. The relatively high $(OC/EC)_{min}$ values for the major warm season trajectories (C-1, C-2 and C-4) suggest a linkage with VOCs and SOC that varies with season.

The westerly C-6 trajectories, which are common in winter, had a $(OC/EC)_{min}$ of 1.9, and this may reflect wintertime biomass burning in the region and in areas to the west (Qu et al., 2008). The $(OC/EC)_{min}$ value for the northwesterly C-7 trajectories from inland Eurasia was 1.3 and thus the lowest of the clusters; this value also is similar to that (1.4) for the polluted transport pathways to Lianyungang, a city near the coast in Eastern China (Zhang et al., 2005) and also in the same range as reported for the Pearl Delta River region of China (Cao et al., 2003).

A summary of the calculated $OC_{pri}$ [$OC_{pri} = OC_{total} - SOC \approx (OC/EC)_{min} * EC$] and SOC concentrations for the five major trajectory clusters shows that the $OC_{pri}$ concentration (1.2 μg $m^{-3}$) and its contribution to $PM_{10}$ mass (12%) were highest for the polluted C-2 trajectories (Table 1). In comparison, low $OC_{pri}$ levels were found for the clean (C-1 and C-4) transport pathways. The relative contribution of EC to $PM_{10}$ mass was highest for the C-3 polluted trajectories (5.3%), consistent with the notion that EC is a primary pollutant and that some OC forms heterogeneously.

The contributions of SOC to $PM_{10}$ mass were generally lower for the short-distance C-2 and C-3 trajectories compared with the longer ones, i.e. C-5, C-6 and C-7 (Table 1). There were relatively high proportions of SOC for the short-distance C-1 and C-4 trajectories (34.5% and 30.9%); but this was probably another effect of seasonality because these trajectories mainly occurred in summer and autumn when SOC formation is efficient (Qu et al., 2008). The relatively constant contribution of EC to $PM_{10}$ mass (4.2%–4.3%) for the long-

**Table 1**
Estimated secondary organic carbon (SOC) aerosols and proportions of carbonaceous aerosols in $PM_{10}$ for bulk aerosol particles under different air-mass trajectory cluster at Zhuzhang (ZUZ) during summer, 2004 to spring, 2005.

| Trajectory cluster | Mean concentration, μg $m^{-3}$ | | SOC proportion in total OC, % | Proportion in $PM_{10}$, % | | |
|---|---|---|---|---|---|---|
| | $OC_{pri}$ | SOC | | $OC_{pri}$ | SOC | EC |
| 2 | 1.2 | 2.4 | 67.5 | 12.0 | 25.6 | 3.9 |
| 3 | 0.58 | 2.8 | 83.0 | 5.7 | 28 | 5.3 |
| 5 | 0.59 | 3.0 | 82.8 | 6.4 | 31.5 | 4.3 |
| 6 | 0.65 | 2.4 | 78.7 | 7.8 | 29.8 | 4.2 |
| 7 | 0.44 | 2.7 | 86.3 | 5.5 | 35.0 | 4.3 |
| 1 | 0.49 | 2.5 | 84.0 | 6.5 | 34.5 | 3.9 |
| 4 | 0.48 | 2.3 | 83.6 | 6.0 | 30.9 | 3.6 |

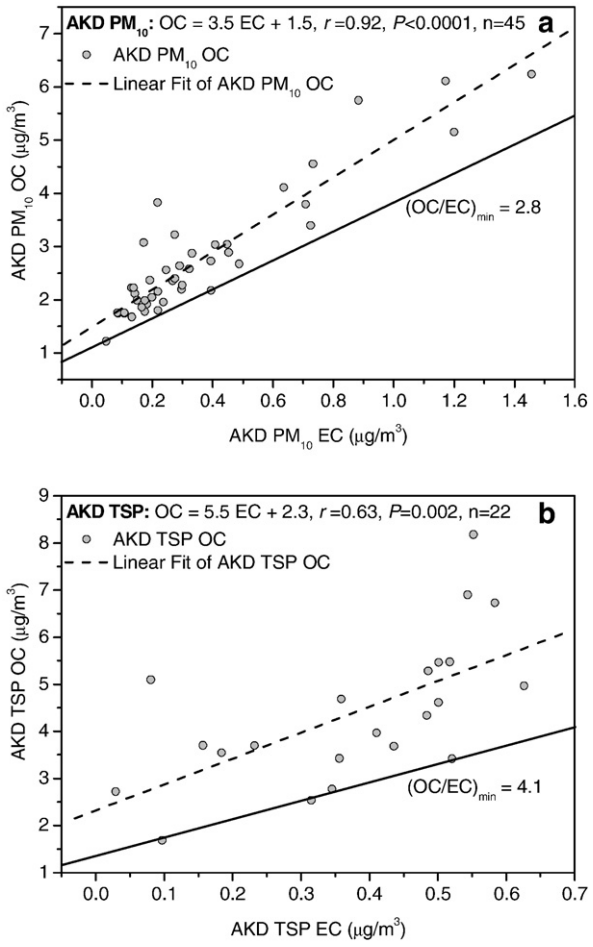


**Fig. 3.** The relationship between organic carbon (OC) and elemental carbon (EC) in $PM_{10}$ (a) and in TSP (b) at Akdala (AKD).

range C-5, C-6 and C-7 transport pathways suggests a relatively well-mixed, stable component of the aerosol.

*3.1.2.2. Secondary organic carbon at Akdala.* Compared with ZUZ, the atmospheric transport pathways to AKD were more similar throughout the year; and therefore, the SOC estimation for AKD was based on the full dataset. There was a significant correlation between OC and EC in $PM_{10}$ at AKD (Fig. 3a), and the $(OC/EC)_{min}$ value (2.8) was similar to the OC/EC ratio reported for $PM_{2.5}$ from residential coal combustion (2.7, Watson et al., 2001), which is one of major regional sources of pollution (Cao et al., 2006). A significant correlation ($p = 0.005$ significance) also was found between OC and EC in TSP, with an $(OC/EC)_{min}$ value of 4.1 (Fig. 3b), which is the same as the OC/EC ratio reported for $PM_{2.5}$ from residential wood combustion (Watson et al., 2001). The higher $(OC/EC)_{min}$ value for TSP compared with $PM_{10}$ implies different OC origins for the coarser and finer particles.

The concentrations of $OC_{pri}$, SOC and their proportions of OC in both $PM_{10}$ and TSP are summarized in Table 2. The fact that $OC_{pri}$ exhibited its highest concentration in winter, suggests regional influences from domestic heating (Qu et al., 2008). Compared with winter and spring, SOC exhibited higher concentrations and commensurately larger proportions of $PM_{10}$ OC in summer and autumn (Table 2); this was probably due to higher summertime OH radical concentrations and photochemistry that was more favorable to SOC formation. The SOC contribution to $PM_{10}$ mass varied in a similar fashion. Secondary aerosol, including SOC, typically is concentrated in the fine particles, and consistent with this, the proportion of OC attributable to SOC at AKD was higher for $PM_{10}$ than TSP. In contrast to the aerosol OC, the proportion of EC in $PM_{10}$ mass was uniform over the different seasons (~3.5%), suggesting a constant EC contribution to aerosol mass in this background region.

The proportions of SOC in OC were relatively large at both sites, averaging ~81% at ZUZ and ~68% at AKD. As a major constituent of the aerosol, SOC accounted for 26% to 35% of $PM_{10}$ mass at ZUZ and 13 to 35% at AKD (Tables 1 and 2). These values are comparable to or slightly lower than SOC contributions reported for other background areas. For instance, SOC accounted for $66.7 \pm 11.9\%$ of $PM_{2.5}$ OC in October 2001 for a agricultural and pasturing area in California (Kwangsam et al., 2004); similarly, SOC composed of 40% to 80% of $PM_{2.5}$ OC in summer 1987 at Claremont, US (Turpin and Huntzicker, 1995). At a coastal rural site in Portugal, SOC made up 78% of the OC in marine air parcels (Castro et al., 1999). As noted above, large proportions of SOC at background sites generally can be explained by the formation of SOCs during transport.

*3.1.3. Frequency distributions of OC, EC concentrations and OC/EC ratios*

Examination of the statistical distributions of mass concentrations and aerosol components provides information on the variance in the aerosol populations. The OC and EC concentrations and OC/EC ratios in $PM_{10}$ all plotted as positively skew distributions at ZUZ and AKD (Fig. 4); the modal OC concentrations were 3.1 μg $m^{-3}$ at ZUZ and 1.9 μg $m^{-3}$ at AKD. The modal EC concentration was 0.35 μg $m^{-3}$ at ZUZ; while at AKD the EC concentrations showed bimodal frequency distribution, one peak at ~0.15 μg $m^{-3}$ presumably reflecting the background conditions, and the other ~0.7 μg $m^{-3}$ representing the EC levels during more polluted episodes (Fig. 4e). The frequency distribution of OC/EC ratios revealed a modal OC/EC ratio of 7.5 at ZUZ and a lower modal ratio of 6.5 at AKD (Fig. 4c and f); the lower ratio at AKD presumably reflects the transport of pollution as discussed in detail below.

*3.1.4. Relationships between OC/EC ratios and EC concentrations*

A curve fitted to the ZUZ data (Fig. 4g) shows that as the EC concentrations increased, the OC/EC ratios approached a constant value of ~7.5; indeed, the first-order, exponential-decay fit between

**Table 2**
Estimated secondary organic carbon (SOC) aerosols and proportions of carbonaceous aerosols in $PM_{10}$ and in TSP for bulk aerosol particles at Akdala (AKD) during summer, 2004 to spring, 2005.

| | Season | n[a] | Mean concentration, μg $m^{-3}$ | | SOC proportion in total OC, % | Proportion in $PM_{10}$, % | | |
|---|---|---|---|---|---|---|---|---|
| | | | $OC_{pri}$ | SOC | | $OC_{pri}$ | SOC | EC |
| $PM_{10}$ | Aug, 2004 | 5 | 0.52 | 2.0 | 79.1 | 8.0 | 31.7 | 2.9 |
| | Sep and Nov, 2004 | 10 | 0.70 | 1.8 | 77.6 | 8.6 | 34.9 | 3.1 |
| | Winter, 2004 | 27 | 1.3 | 1.7 | 61.3 | 8.5 | 13.3 | 3.1 |
| | Mar, 2005 | 4 | 0.45 | 1.4 | 76.0 | 8.3 | 26.9 | 3.0 |
| | Whole sampling period | 46 | 0.99 | 1.8 | 68.2 | 8.5 | 21.4 | 3.1 |
| TSP | Jul and Aug, 2004 | 13 | 1.7 | 3.1 | 63.2 | | | |
| | Sep, 2004 | 9 | 1.3 | 2.4 | 66.1 | | | |
| | Whole sampling period | 22 | 1.6 | 2.8 | 64.4 | | | |

[a] Here, *n*, number of samples.

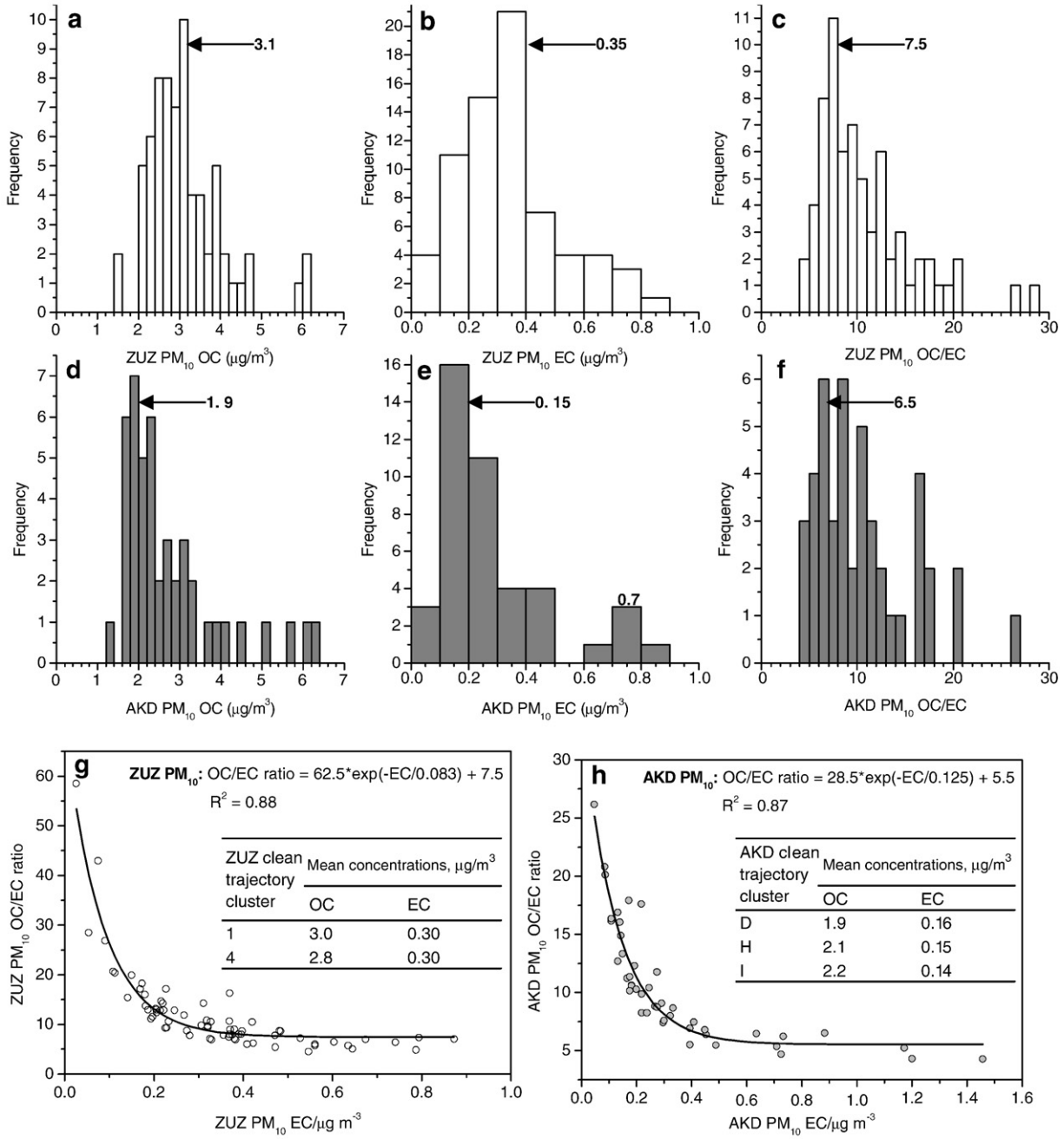


**Fig. 4.** Frequency distribution of (a) organic carbon (OC) concentration, (b) elemental carbon (EC) concentration and (c) OC/EC ratio in $PM_{10}$ at Zhuzhang (ZUZ); frequency distribution of (d) OC concentration, (e) EC concentration and (f) OC/EC ratio in $PM_{10}$ at Akdala (AKD); first order exponential decay fitting between $PM_{10}$ OC/EC ratio and EC concentration at ZUZ (g) and AKD (h). Mean concentrations of OC and EC for the clean trajectory clusters at ZUZ (g) and AKD (h) are also presented.

the OC/EC ratios and $PM_{10}$ EC concentrations has an $R^2$ value of 0.88. This asymptote is similar to the modal OC/EC ratio (Fig. 4c), and it also is similar to the OC/EC ratio of 6.6 found for the polluted C-3 trajectories, which is the cluster that had the highest EC concentration.

Fig. 4g also shows that as the OC/EC ratios increased, the EC concentrations approached a minimum, possibly reflecting the EC concentrations in the absence of regional pollutants, and thus the regional background. The low EC concentrations for the clean C-1 and C-4 trajectories to ZUZ (both 0.30 μg $m^{-3}$, Fig. 1) also suggest an EC background value. Moreover, as was the case for EC, the OC concentrations for the clean C-1 and C-4 ZUZ trajectories were the lowest of all the transport clusters, averaging 3.0 μg $m^{-3}$ and 2.8 μg $m^{-3}$. The OC and EC concentrations for the two clean trajectory clusters also were similar to the modal OC and EC concentrations shown in Fig. 4a and b. Therefore, C-1 and C-4 pathways, which accounted for 42% of the trajectories and ostensibly tracked marine air that had passed over a coastal area around Bay of Bengal, may best reflect the aerosol background at ZUZ.

Similarly, the first-order, exponential-decay fit between the OC/EC ratios and $PM_{10}$ EC concentrations at AKD has an $R^2$ value of 0.87; and the fitted curve (Fig. 4h) indicated that as EC concentrations increased, the OC/EC ratios approached a constant value of 5.5. This is comparable to the modal OC/EC ratio (Fig. 4f) and to the OC/EC ratio of 5.7 found for the polluted C-J trajectories, the group with the highest EC concentrations. In Fig. 4h one also can see that as OC/EC ratios increased, the EC concentrations approached a minimum, possibly representing the regional background. The low EC concentrations for the clean C-D, C-H and C-I AKD trajectories (~0.15 μg $m^{-3}$, Fig. 1) and the low modal EC

value (0.15 μg $m^{-3}$, Fig. 4e) support this contention. Moreover, as was the case for EC, the OC concentrations for the clean trajectories (C-D, C-H and C-I) were the lowest of all the transport clusters; the OC averages for these clusters ranged in 1.9–2.2 μg $m^{-3}$, similar to the modal OC concentration (Fig. 4d). Therefore, C-D, C-H and C-I pathways, although accounting only for 7% of the trajectories, may best represent the aerosol background at AKD.

### 3.2. Differences in the aerosol populations at Zhuzhang and Akdala

#### 3.2.1. Central tendencies and variations of the aerosol concentrations

At AKD the arithmetic mean concentrations of OC, EC, $SO_4^{2-}$, $NO_3^-$, $NH_4^+$ and soil dust were considerably higher than their medians (Fig. 5, Table 3). These differences in the aerosol populations (except soil dust) presumably result from the high concentrations that occurred during pollution episodes and caused the skewness in the distributions. Here, the soil dust fraction was estimated based on the 4% elemental Fe content of dust samples from the Mu Us Desert (Zhang et al., 2003), a value also similar to that in the earth's upper continental crust. Note that soil dust is mostly natural in origin and normally would not be greatly influenced by pollution episodes; however, its levels evidently can be elevated during dust events as this region is adjacent to some large dust sources.

In contrast, at ZUZ, the arithmetic mean concentrations of OC, EC, $SO_4^{2-}$, $NO_3^-$, $NH_4^+$ and soil dust were much more comparable to their medians. This suggests weaker influences from pollution, and a more stable aerosol background. Because there are inevitably some pollution events at most sampling sites, the identification of the data with the least perturbation is a way to characterize atmospheric backgrounds.

Indeed, the frequency distributions of the 30-minute averaged ambient $PM_{10}$ mass concentrations measured synchronously during the sampling course illustrated strongly skew-right distributions at AKD compared with more symmetrical ones at ZUZ (Fig. 5g and h). Comparisons of the real-time $PM_{10}$ mass concentrations also indicated that AKD was more likely influenced by pulses of aerosol pollution than ZUZ. Finally, it is worth noting that the modal real-time $PM_{10}$ mass concentrations (3.5 to 5.0 μg $m^{-3}$ at ZUZ and 4.0 to 10 μg $m^{-3}$ at AKD, respectively) were comparable with the gravimetrically determined $PM_{10}$ concentrations at both sites.

Comparisons between the sites show that $SO_4^{2-}$, $NH_4^+$, $NO_3^-$ and soil dust had significantly higher mean concentrations and median concentrations at AKD than at ZUZ (Fig. 5, Table 3). On other hand, although there were similar arithmetic mean OC and EC concentrations (in the ranges of 2.9–3.1 μg $m^{-3}$ and 0.34–0.35 μg $m^{-3}$, respectively) at the two sites, the median OC and EC concentrations at AKD (2.4 and 0.24 μg $m^{-3}$) were lower than those at ZUZ (3.0 and 0.32 μg $m^{-3}$) (Fig. 5, Table 3).

Variations in the aerosol populations, can be further evaluated by comparing the interquartile ranges (IQRs), that is, the difference between the 75th and 25th percentile values. The IQRs were used here

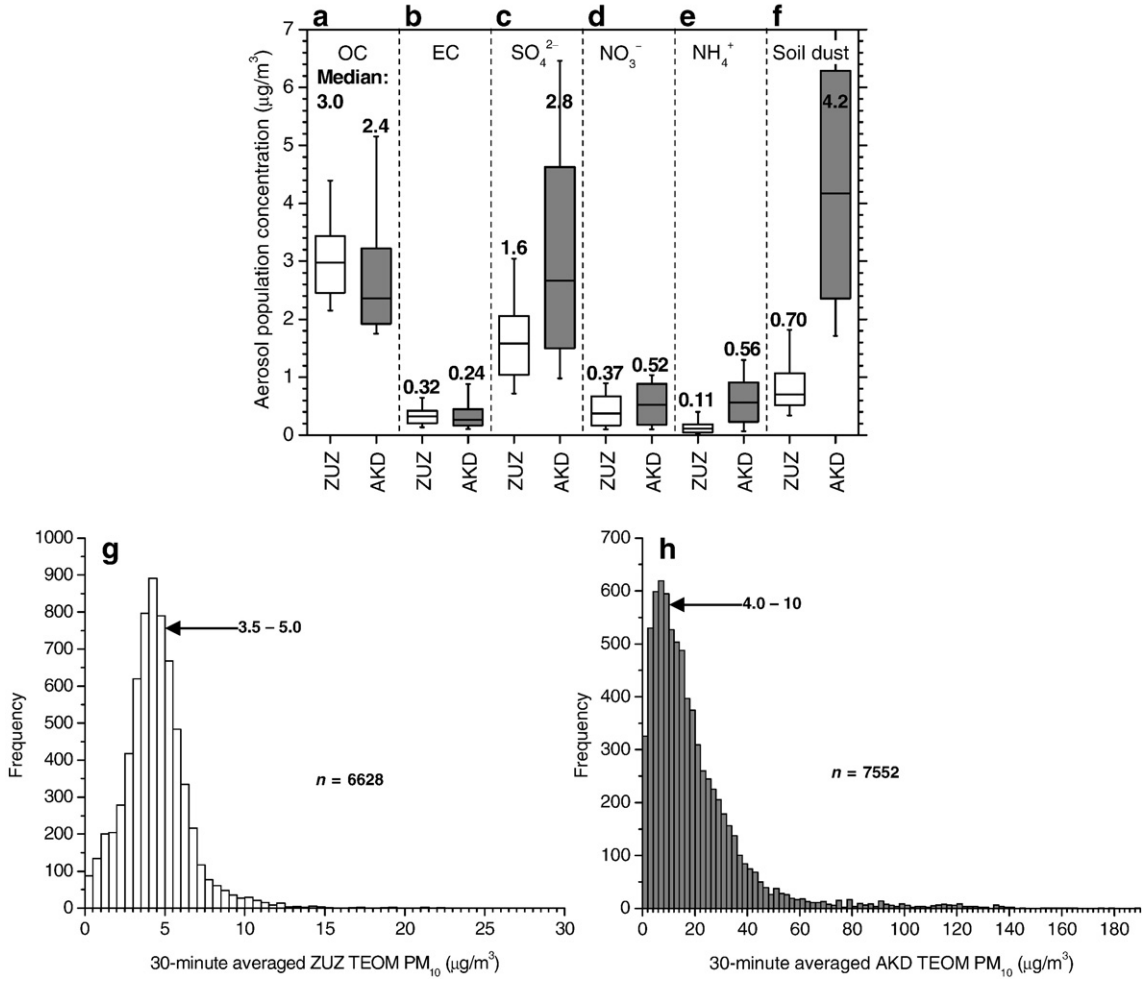


**Fig. 5.** Median and variation of 3-day averaged (a) organic carbon (OC), (b) elemental carbon (EC), (c) sulfate ($SO_4^{2-}$), (d) nitrate ($NO_3^-$), (e) ammonium ($NH_4^+$), and (f) soil dust concentrations in $PM_{10}$ from August 2004 to February 2005 at Zhuzhang (ZUZ) and Akdala (AKD); the box-and-stem plots depict the 10th, 25th, 50th, 75th, and 90th percentile for the concentrations of aerosol populations; the median 50th percentile concentrations are also presented. Frequency distributions of the on-line observed 30-minute averaged $PM_{10}$ concentrations by using TEOM® series 1400a ambient particulate monitor (Rupprecht & Patashnick, US) during the sampling course at ZUZ (g) and AKD (h).

**Table 3**
Median and mean concentrations of the aerosol populations in $PM_{10}$ during summer, 2004 to spring, 2005 at Zhuzhang (ZUZ) and Akdala (AKD).

| Aerosol populations | ZUZ concentration, μg $m^{-3}$ | | | AKD concentrating, μg $m^{-3}$ | | |
|---|---|---|---|---|---|---|
| | $n$[a] | Median | Arithmetic mean ± standard deviation | $n$ | Median | Arithmetic mean ± standard deviation |
| OC | 70 | 3.0 | 3.1 ± 0.91 | 45 | 2.4 | 2.9 ± 1.6 |
| EC | 70 | 0.32 | 0.34 ± 0.18 | 45 | 0.24 | 0.35 ± 0.31 |
| $SO_4^{2-}$ | 74 | 1.6 | 1.6 ± 0.77 | 56 | 2.8 | 3.3 ± 2.1 |
| $NO_3^-$ | 74 | 0.37 | 0.45 ± 0.34 | 56 | 0.52 | 0.58 ± 0.45 |
| $NH_4^+$ | 71 | 0.11 | 0.15 ± 0.14 | 53 | 0.56 | 0.60 ± 0.42 |
| Soil dust[b] | 69 | 0.70 | 0.85 ± 0.57 | 17[c] | 4.2 | 4.7 ± 2.4 |

[a] Here, $n$, number of samples.
[b] Estimated based on 4% elemental Fe content of dust samples from the Mu Us Desert (Zhang et al., 2003).
[c] Soil dust data are only available from later July to early September 2004 at AKD.

because they reflect variations in centers of the distributions, rather than the standard deviations which measure the average dispersions of all data points from the mean. These comparisons indicated that OC, EC and $NO_3^-$ were slightly more variable at AKD, that is, the IQRs were about 10 to 40% higher than those at ZUZ. However, much larger variations were observed for $SO_4^{2-}$, $NH_4^+$ and soil dust at AKD; for these analytes, the IQRs were about three to seven times those at ZUZ. Thus, the spread in the aerosol populations' concentrations was considerably narrower at ZUZ than at AKD (Fig. 5); this further implies that ZUZ is more often representative of regional background conditions than AKD.

The variability exemplified by the IQRs and the box and stem plots reflects variations in source emissions, meteorological processes as well as pollutant transport. Larger variations in most of the aerosols at AKD implied stronger impacts of pollution on background levels, and this may be due to the transport of upwind pollution from Russia (see C-J and C-G trajectories, Fig. 1). Meanwhile, AKD also experiences more soil dust released from the Gobi and adjacent deserts. In contrast, although OC and EC concentrations were slightly more variable at AKD, their median concentrations were lower than at ZUZ (Fig. 5a and b); suggesting that there may be lower background levels of carbonaceous aerosol in the mid-latitude area where AKD is located. Slightly higher and more stable OC and EC background levels were observed in the low latitude area where ZUZ is situated, probably due to regional anthropogenic emissions as well as the input of pollutants upwind which are often mid- to high latitude areas.

The contributions of the major components to the total aerosol mass differed between ZUZ and AKD: for example, the proportions of OC, $SO_4^{2-}$ and EC in $PM_{10}$ were about 47%, 24% and 5.1% at ZUZ compared with 29%, 34% and 3.5% at AKD (Qu et al., 2008). The concentrations of OC are less variable than most of the other aerosol species, and OC contributes significantly to the aerosol mass at these two sites; EC on the other hand is lower at the mid- to high latitude area (AKD), but its concentration increases during pollution events. In general, the higher EC mass fraction at ZUZ compared to AKD implies that the aerosol population over the remote low latitude area is more absorbing than that over the remote mid- to high latitude area in western China. These differences in background aerosol and pollution impacts presumably lead to different regional radiative effects and so may have important implications for regional climate.

### *3.2.2. Organic carbon/elemental carbon ratios as indicators of background versus polluted conditions*

Inspection of the data showed opposing temporal trends in the OC/EC ratios and $PM_{10}$ TC concentrations at both sites. Low OC/EC ratios occurred during pollution episodes, that is when EC was elevated, while the increases in OC/EC ratios are most easily explained by SOC formation during transport, along with the mixing, diffusion and dilution of the primary pollutants such as EC. This latter case provides useful information on the background aerosol. Therefore, we evaluated changes in OC/EC ratios as a means of distinguishing background conditions from those influenced by polluted events.

For this analysis, we divided the data into two subsets, i.e. samples with OC/EC ratios higher than its total median value and those with lower OC/EC ratios (Fig. 6a and d). The hypothesis to be tested was that the high-ratio subgroup mainly consisted of samples collected during clean periods (hereinafter referred to as "background samples") while the low-ratio group included samples collected during polluted episodes ("polluted samples"). Note that this separation is particularly sensitive to the formation of SOC, and therefore the aerosol concentrations of the background samples were generally, but not necessarily, lower than those for the polluted samples. Furthermore, the background samples cannot be expected to be totally free from anthropogenic influences, but we did find this approach helpful in assessing the aerosol backgrounds at the two sites.

At ZUZ, the modal OC/EC ratios were 12.5 and 7.5 for the background samples and the polluted samples, respectively (Fig. 6a) while at AKD the corresponding modal ratios were 10.5 and 6.5 (Fig. 6d). The modal OC/EC ratios were evaluated here instead of the means because the distributions were non-normal, and the modes reflect the most frequently observed conditions. The OC/EC ratios for the polluted samples were not only lower but also less variable compared with the background samples at both sites. Although significant correlations ($p<0.001$ significance) were found between OC and EC in $PM_{10}$ for both the background samples and the polluted samples, the correlations for the background dataset ($r=0.75$ for ZUZ and $r=0.69$ for AKD, Fig. 6b and e) were less than those for the polluted dataset ($r=0.84$ for ZUZ and $r=0.95$ for AKD, Fig. 6c and f). This suggests that the influences of the primary sources were more important for the polluted samples while SOC formation more strongly affected the ratios of the background samples.

The median concentrations of OC, EC, $SO_4^{2-}$, $NH_4^+$ and soil dust (but not $NO_3^-$) were higher in the ZUZ $PM_{10}$ samples that were classified as polluted on the basis of OC/EC ratios (Fig. 7a, b, c, e and f). The IQRs for these species in the polluted group were 1.3 to 2.2 times those of the background samples, indicating greater variability during pollution events. In contrast, the two ZUZ subgroups exhibited similar $NO_3^-$ median concentrations with IQR in the polluted group only 0.6 times that of the background group, which was probably due to efficient transport (Chow et al., 1998, 2002) and possibly a more homogeneous spatial distribution of this secondary aerosol in the region. At AKD, the median concentrations of OC, EC, $SO_4^{2-}$, $NO_3^-$ and $NH_4^+$ also differed between the groups split on the basis of OC/EC ratios (Fig. 7g, h, i, j and k), soil dust was not included here because of incomplete data. The IQRs for $SO_4^{2-}$, $NO_3^-$ and $NH_4^+$ for polluted AKD samples were slightly higher than those in the clean group, but the IQRs for OC and EC were about 3.0 and 6.7 fold higher in the polluted samples.

The data stratified by OC/EC ratios show that the concentrations of OC, EC, $SO_4^{2-}$, $NO_3^-$ and $NH_4^+$ increased more during pollution episodes at AKD compared with ZUZ, and this is consistent with the greater influences of pollution emission on air quality at AKD. These results show that OC/EC ratios can be used as a means of distinguishing polluted periods from background conditions at our two background sites. That is, higher OC/EC ratios are more representative of regional background, whereas pollution emissions tend to drive the ratios lower. Further investigations are necessary to determine the general applicability of this approach for evaluating pollution levels at remote sites.

### *3.2.3. Differences in OC/EC background levels at the two sites*

The EC background level at ZUZ in southwestern China was ~0.30 μg $m^{-3}$, whereas that in northern Xinjiang Province where AKD is located was ~0.15 μg $m^{-3}$. One possible explanation for this difference is that the anthropogenic emissions are comparatively

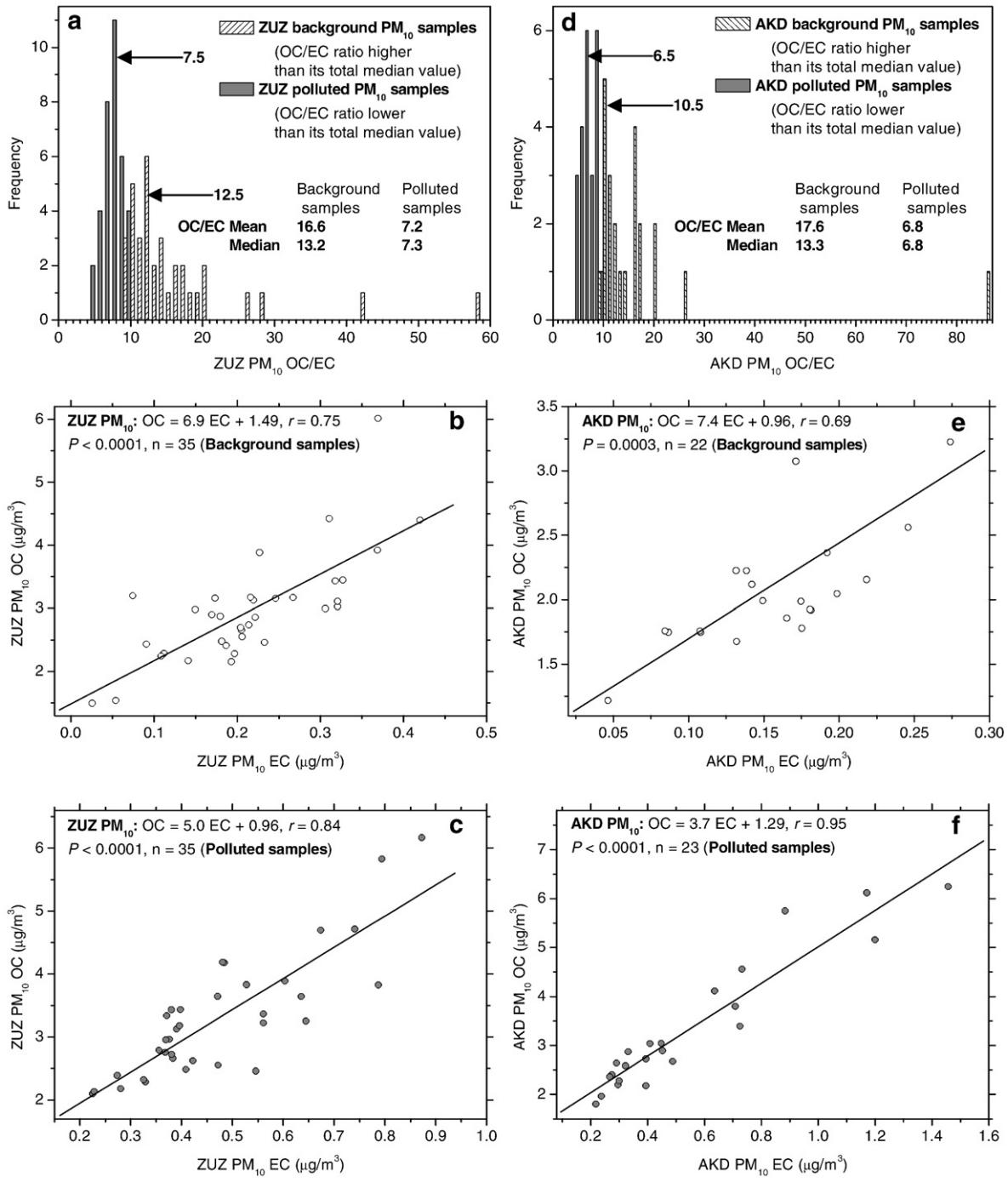


**Fig. 6.** Frequency distribution of (a) OC/EC ratio in $PM_{10}$ at Zhuzhang (ZUZ), (d) OC/EC ratio in $PM_{10}$ at Akdala (AKD) for the background samples (OC/EC ratio higher than its total median value) and the polluted samples (OC/EC ratio lower than its total median value); OC and EC relationship in $PM_{10}$ at ZUZ for (b) the background samples and (c) the polluted samples; OC and EC relationship in $PM_{10}$ at AKD for (e) the background samples and (f) the polluted samples.

weaker in the mid- to high latitude area. On the other hand, the mid- to high latitude sources in Eurasia are upwind of the low latitude ZUZ area, and so pollutants could easily have been transported to that site. Observations at Mt. Waliguan have shown that the monthly average EC concentrations from 1994 to 1995 were 0.13 to 0.3 μg $m^{-3}$ (Tang et al., 1999), similar to what we measured at AKD and ZUZ in what was presumed to be background air. In contrast, the EC concentrations reported for the Lin'an regional background station ($2.5 \pm 0.7$ to $3.4 \pm 1.7$ μg $m^{-3}$, Xu et al., 2002; Wang et al., 2004) are much higher than those at Mt. Waliguan or the sites we sampled. Lin'an is in Zhejiang Province, a heavily populated area in southeastern China and it is subject to strong anthropogenic emissions.

The OC background concentrations at ZUZ (2.8 to 3.0 μg $m^{-3}$) and AKD (1.9 to 2.2 μg $m^{-3}$) were comparable with those measured over the sea surface near South Korea in August 1994 ($2.36 \pm 0.16$ μg $m^{-3}$, Kim et al., 1999). In contrast, the EC background concentrations at ZUZ (0.30 μg $m^{-3}$) and at AKD (0.15 μg $m^{-3}$) were higher than those reported for the same South Korean study ($0.08 \pm 0.02$ μg $m^{-3}$) and also higher than EC background concentration of 0.09 μg $m^{-3}$ over the northwest Pacific during March to April, 2001 reported by Lim et al. (2003); this difference in EC levels was presumably due to stronger anthropogenic influences over the continents compared with the sea.

The differences in background EC and OC levels and their contributions to the total aerosol reported here may result in different

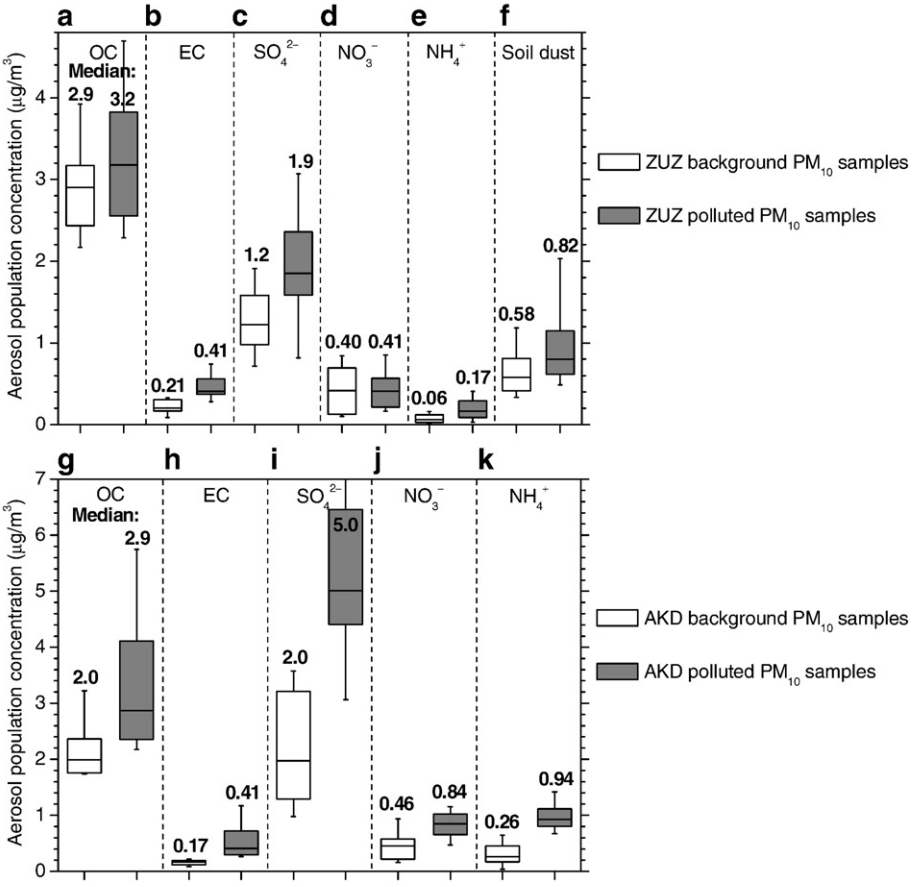


**Fig. 7.** Median and variation of 3-day averaged (a) organic carbon (OC), (b) elemental carbon (EC), (c) sulfate ($SO_4^{2-}$), (d) nitrate ($NO_3^-$), (e) ammonium ($NH_4^+$), (f) soil dust concentrations in $PM_{10}$ at Zhuzhang (ZUZ) for the background samples and the polluted samples; median and variation of 3-day averaged (g) OC, (h) EC, (i) $SO_4^{2-}$, (j) $NO_3^-$, (k) $NH_4^+$ concentrations in $PM_{10}$ at Akdala (AKD) for the background samples and the polluted samples from August 2004 to February 2005. The box-and-stem plots depict the 10th, 25th, 50th, 75th, and 90th percentile for the concentrations of aerosol populations. The median 50th percentile concentrations for each group are also presented.

regional effects on climate. For example, Menon et al. (2002) reported that absorbing aerosols such as black carbon (BC, similar to EC, differing mainly in the analytical/determination method) can heat the air, alter regional atmospheric stability and vertical motions, and affect large-scale circulation and the hydrologic cycle; their modeling research suggests that low-level heating due to absorbing aerosols can enhance rising motions locally, resulting in local cooling and enhanced precipitation, with counterbalancing subsidence, warming and decreased rainfall away from the region impacted by the aerosols. These effects of increasing BC aerosol loads have been linked to changes in precipitation trends in China over the past several decades, with increased rainfall and summer floods in the south and drought in the north; changes in aerosol loadings also have been linked to changes in precipitation patterns over India and increased droughts in northern areas such as Afghanistan (Menon et al., 2002). Identification of the difference in background EC levels between the mid- to high latitude areas and the low latitude areas in western China through our studies suggests the regional heterogeneity of this absorbing aerosol needs to be considered when evaluating its regional climate effects.

Our results are consistent with other studies of the spatial distributions of carbonaceous aerosols. For example, based on data collected during four cruises over the western Pacific, Sugimoto et al. (2001) concluded that aerosol density was generally high at latitudes above 25°N where the westerly winds from the Asian continent prevailed, and that the aerosols in the continental air mass were clearly different from those at lower latitudes. From observations over the Arabian Sea, tropical Indian Ocean and Southern Ocean, Moorthy et al. (2005) reported that large latitudinal BC gradients exist north of ~20°S with BC increasing to concentrations as high as 2 μg $m^{-3}$ over the Arabian Sea (~8°N); on the other hand, the fraction of the aerosol mass made up by BC showed a distinctly different variation, with a peak close to the equator and decreasing on either side; this study also showed that BC remained at extremely low (<0.05 μg $m^{-3}$) and remarkably constant concentrations over the Southern Ocean (20°S to 56°S). It has been suggested that heating caused by high BC loadings in the lower troposphere could result in rising motions of the atmosphere (Menon et al., 2002); such effects by relatively higher BC loadings in the low latitude presumably could contribute to large-scale effects on atmospheric circulation (Hu and Fu, 2007; Seidel et al., 2008).

## 4. Conclusions

(1) High OC/EC ratios and large proportions of SOC in the total aerosol OC were found at ZUZ and AKD; this is best explained by the formation of SOC during transport. In general, the large proportion of OC in these Chinese background aerosols may result in a stronger cooling effect compared with the warming from EC, but this suggestion obviously needs to be verified through measurements.

In comparison, the spatial distribution of EC is apparently more patchy than OC, and at these remote Chinese background sites, the EC concentrations are low (~0.15 to ~0.3 μg $m^{-3}$). Along these lines, observations in the San Joaquin Valley and in the Valle de Mexico (Chow et al., 1998, 2002) have revealed efficient regional transport (for hundreds of kilometers) of particulate sulfate, nitrate and OC (which contain large secondary proportion resulted from photochemical conversion) compared with a more restricted spatial distribution of EC (transport less than 1 to 5 km). Therefore, in regions lacking

strong anthropogenic emissions, OC generally will contribute more to the carbonaceous aerosol population than EC. Even so, high EC levels in some large Chinese cities have the potential to cause adverse health effects in addition to any effects on climate.

SOC accounted for 26 to 35% of the $PM_{10}$ mass at ZUZ versus 13 to 35% at AKD. A relatively constant EC contribution to $PM_{10}$ mass (4.2% to 4.3%) for the long-range transport pathways to ZUZ as well as a similar proportion of EC in $PM_{10}$ mass over the different seasons (~3%) at AKD indicates that EC is a relatively constant component in these regional background aerosols. As SOC was found to contribute the most mass to the carbonaceous aerosol, reducing emissions of VOCs and the precursor gases of SOC (e.g. hydrocarbon) would be an efficient way of reducing PM levels in China.

(2) OC/EC ratios were used to distinguish polluted periods from background conditions. The frequency distributions of OC and EC, first order exponential decay fitting relationship between OC/EC ratio and EC concentration, combined with estimates of the pollutants' levels for the transport pathways indicated that background EC and OC concentrations in $PM_{10}$ were ~0.30 μg $m^{-3}$ and 2.8 to 3.0 μg $m^{-3}$ at ZUZ, in contrast to ~0.15 μg $m^{-3}$ and 1.9 to 2.2 μg $m^{-3}$ at AKD.

The higher EC background concentration and the greater contribution of EC to the total aerosol mass at the low latitude ZUZ site compared with the mid-latitude AKD site can be explained by stronger regional anthropogenic emissions combined with greater inputs of pollutants upwind. The latter often originate from mid- to high latitude areas, and their transport is driven by the monsoonal circulation in Eurasia. Similarly, differences in the background levels and contributions of the crucial aerosol components (such as OC, EC, sulfate and soil dust) to the total aerosol between AKD and ZUZ presumably lead to different regional radiative effects, and these should be taken into account when assessing perturbations to regional climate.

It is likely that efficient mixing upwind may result in a comparatively consistent aerosol mixture and a relatively constant aerosol background in the low-latitude Eurasian background area like ZUZ. However, this contention needs further investigation.

(3) Unlike the relatively similar levels of OC and $NO_3^-$ (which also has an important secondary fraction) in the "background " and "polluted samples", other aerosol species, including EC, $SO_4^{2-}$, $NH_4^+$, and soil dust, increased by factors of 1.4 to 2.6 from their background conditions during polluted episodes at ZUZ. At AKD, OC, EC, $SO_4^{2-}$, $NO_3^-$ and $NH_4^+$ all exhibited higher concentrations with larger variations during polluted conditions. Because of the inevitable occurrence of pollution impacts, identification of the data with the least perturbation is essential for determining background conditions.

Atmospheric data available from remote sites in China are still quite limited, and future work should focus on extending the coverage of background observations and improving the representativeness of these observations. Better information on the aerosol background for different regions of the country will be valuable for assessing the aerosols' regional climate effects and for implementing the air pollution control strategies in China.

## Acknowledgments

This research was supported by National Basic Research Program of China (Grant No. 2006CB403701, 2006CB403702) and by the National Science Foundation of the United States (ATM 0404944). We are grateful to the members of CAWAS at Chinese Academy of Meteorological Sciences for their support, dedication, and many contributions to our project.

## References

Arimoto R, Snow JA, Graustein WC, Moody JL, Ray BJ, Duce RA, et al. Influences of atmospheric transport pathways on radionuclide activities in aerosol particles from over the North Atlantic. J Geophys Res 1999;104:21301–16.

Cachier H, Brémond MP, Buat-Ménard P. Carbonaceous aerosols from different tropical biomass burning sources. Nature 1989;340:371–3.

Cao GL, Zhang XY, Zheng FC. Inventory of black carbon and organic carbon emissions from China. Atmos Environ 2006;40:6516-26527.

Cao JJ, Lee SC, Ho KF, Zhang XY, Zou SC, Fung K, et al. Characteristics of carbonaceous aerosol in Pearl River Delta Region, China during 2001 winter period. Atmos Environ 2003;37:1451–60.

Castro LM, Pio CA, Harrison RM, Smith DJ. Carbonaceous aerosol in urban and rural European atmospheres: estimation of secondary organic carbon concentrations. Atmos Environ 1999;33:2771–81.

Chow JC, Waston JG, Pritchett LC, Pierson WR, Frazier CA, Purcell RG. The DRI thermal/optical reflectance carbon analysis system: description, evaluation and applications in US air quality studies. Atmos Environ 1993;27A:1185–201.

Chow JC, Watson JG, Lowenthal DH, Egami RT, Solomon PA, Thuillier RH, et al. Spatial and temporal variations of particulate precursor gases and photochemical reaction products during SJVAQS/AUSPEX ozone episodes. Atmos Environ 1998;32:2835–44.

Chow JC, Watson JG, Edgerton SA, Vega E. Chemical composition of $PM_{2.5}$ and $PM_{10}$ in Mexico City during winter 1997. Sci Total Environ 2002;287:177–201.

Draxler RR, Hess GD. An overview of the HYSPLIT_4 modelling system for trajectories, dispersion, and deposition. Aust Meteorol Mag 1998;47:295–308.

Duan FK, He KB, Ma YL, Jia YT, Yang FM, Lei Y, et al. Characteristics of carbonaceous aerosols in Beijing, China. Chemosphere 2005;60:355–64.

Ferek RJ, Reid JS, Hobbs PV, Blake DR, Liousse C. Emission factors of hydrocarbons, halocarbons, trace gases and particles from biomass burning in Brazil. J Geophys Res 1998;103(D24):32107–18.

He Z, Kim YJ, Ogunjobi KO, Kim JE, Ryu SY. Carbonaceous aerosol characteristics of $PM_{2.5}$ particles in Northeastern Asia in summer 2002. Atmos Environ 2004;38:1795–800.

Hidy GM, Blanchard CL. The midlatitude North American background aerosol and global aerosol variation. J Air Waste Manage Assoc 2005;55:1585–99.

Highwood EJ, Kinnersley RP. When smoke gets in our eyes: The multiple impacts of atmospheric black carbon on climate, air quality and health. Environ Int 2006;32:560–6.

Hu YY, Fu Q. Observed poleward expansion of the Hadley circulation since 1979. Atmos Chem Phys 2007;7:5229–36.

Kim YP, Moon KC, Lee JH, Baik NJ. Concentrations of carbonaceous species in particles at Seoul and Cheju in Korea. Atmos Environ 1999;33:2751–8.

Kim BM, Teffera S, Zeldin MD. Characterization of $PM_{2.5}$ and $PM_{10}$ in the south coast air basin of Southern California: part 1-spatial variations. J Air Waste Manage Assoc 2000;50:2034–44.

Kwangsam N, Aniket AS, Chen S, David R, Cocker I. Primary and secondary carbonaceous species in the atmosphere of Western Riverside County, California. Atmos Environ 2004;38:1345–55.

Li Y. Characterization and source apportionment of carbonaceous aerosols over Xi'an atmosphere. Master thesis, Graduate school of the Chinese Academy of Sciences, Xi'an; 2004. (in Chinese).

Lim HJ. Semi-continuous aerosol carbon measurements: addressing atmospheric progress of local and global concern. PhD thesis, the Graduate School-New Brunswick Rutgers, State University of New Jersey; 2001.

Lim HJ, Turpin BJ, Russell LM, Bates TS. Organic and elemental carbon measurements during ACE-Asia suggest a longer atmospheric lifetime for elemental carbon. Environ Sci Technol 2003;37:3055–61.

Ma JZ, Tang J, Li SM, Jacobson MZ. Size distributions of ionic aerosols measured at Waliguan Observatory: implication for nitrate gas-to-particle transfer processes in the free troposphere. J Geophys Res 2003;108:4541. doi:10.1029/2002JD003356.

Menon S, Hansen J, Nazarenko L, Luo YF. Climate Effects of Black Carbon Aerosols in China and India. Science 2002;297:2250–3.

Moody JL, Galloway JN. Quantifying the relationship between atmospheric transport and the chemical composition of precipitation on Bermuda. Tellus 1988;40B:463–79.

Moorthy KK, Satheesh SK, Babu SS, Saha A. Large latitudinal gradients and temporal heterogeneity in aerosol black carbon and its mass mixing ratio over southern and northern oceans observed during a trans-continental cruise experiment. Geophys Res Lett 2005;32:L14818. doi:10.1029/2005GL023267.

Qu WJ, Zhang XY, Arimoto R, Wang D, Wang YQ, Yan LW, et al. Chemical composition of the background aerosol at two sites in southwestern and northwestern China: potential influences of regional transport. Tellus 2008;60B:657–73. doi:10.1111/j.1600-0889.2008.00342.x.

Seidel DJ, Fu Q, Randel WJ, Reichler TJ. Widening of the tropical belt in a changing climate. Nat. Geosci. 2008;1:21–4.

Sugimoto N, Matsui I, Liu Z, Shimizu A, Asai K, Yoneyama K, et al. Latitudinal distribution of aerosols and clouds in the western Pacific observed with a lidar on board the research vessel Mirai. Geophys Res Lett 2001;28:4187–90.

Tang J, Wen YP, Zhou LX, Qi DL, Zheng M, Trivett N, et al. Observational study of black carbon in clean air area of western China. Q J Appl Meteorol 1999;10:160–70 (in Chinese).

Turpin BJ, Huntzicker JJ. Secondary formation of organic aerosol in the Los Angeles Basin: a descriptive analysis of organic and elemental carbon concentrations. Atmos Environ 1991;25A:207–15.

Turpin BJ, Huntzicker JJ. Identification of secondary aerosol episodes and quantification of primary and secondary organic aerosol concentrations during SCAQS. Atmos Environ 1995;29:3527–44.

Wang GC, Wen YP, Kong QX, Ren LX, Wang ML. $CO_2$ background concentration in the atmosphere over the Chinese mainland. Chinese Sci Bull 2002;47:1217–20.

Wang T, Wong CH, Cheung TF, Blake DR, Arimoto R, Baumann K, et al. Relationships of trace gases and aerosols and the emission characteristics at Lin'an, a rural site in eastern China, during spring 2001. J Geophys Res 2004;109:D19S05. doi:10.1029/2003JD004119.

Watson JG, Chow JC, James E, Houck E. $PM_{2.5}$ chemical source profiles for vehicle exhaust, vegetative burning, geological material, and coal burning in Northwestern Colorado during 1995. Chemosphere 2001;43:1141–51.
Xu J, Bergin MH, Yu X, Liu G, Zhao J, Carrico CM, et al. Measurement of aerosol chemical, physical and radiative properties in the Yangtze delta region of China. Atmos Environ 2002;36:161–73.
Ye BM, Ji XL, Yang HZ, Yao XH, Chan CK, Cadle SH, et al. Concentration and chemical composition of $PM_{2.5}$ in Shanghai for a 1-year period. Atmos Environ 2003;37:499–510.
Zhang XY, Gong SL, Arimoto R, Shen ZX, Mei FM, Wang D, et al. Characterization and temporal variation of Asian dust aerosol from a site in the northern Chinese deserts. J Atmos Chem 2003;44:241–57.
Zhang XY, Wang YQ, Wang D, Gong SL, Arimoto R, Mao LJ, et al. Characterization and sources of regional-scale transported carbonaceous and dust aerosols from different pathways in coastal and sandy land areas of China. J Geophys Res 2005;110:D15301. doi:10.1029/2004JD005457.
Zhang X.Y., Wang Y.Q., Zhang X.C., Guo W., Gong S. . Carbonaceous Aerosol Composition over Various Regions of China during 2006. J Geophys Res 2008;113:D14111. doi:10.1029/2007JD009525.
Zhou LX, Worthy DEJ, Lang PM, Ernst MK, Zhang XC, Wen YP, et al. Ten years of atmospheric methane observations at a high elevation site in western China. Atmos Environ 2004;38:7041–54.